Identification and Correction of Artifact in the Measurement of Pulsed Magnetic Fields

(Article begins on next page)

27 April 2024

Identification and correction of artefact in the measurement of pulsed magnetic fields

Luca Giaccone, *Senior, IEEE,* Domenico Giordano and Gabiella Crotti

Abstract—**AC magnetic flux density meters usually integrate a high pass filter with a very low cut-off frequency (1 Hz - 30 Hz) aiming at reducing the effect of slow oscillations. This can distort the actual time domain behaviour of magnetic flux density waveforms detectable close to industrial or medical devices, even causing artefact high amplitude oscillations. This paper proposes a procedure to identify the filter parameters that accurately reproduce its measured frequency behaviour and suggests an algorithm to correct, in time domain, the field meter recorded waveform. Identification and correction procedure are extensively tested on magnetic flux density waveforms provided by a system for the generation of standard magnetic fields. Finally, the uncertainty associated with the identification and correction procedure are assessed by means of the Monte Carlo method. Assuming an overall standard uncertainty associated with the MCM model inputs of $0.3\,\%$, a standard uncertainty of $0.75\,\%$ associated with the mean square error between measured and reconstructed waveforms is obtained.**

Index Terms—**Measurement, pulsed magnetic fields, optimisation, identification, dosimetry.**

I. INTRODUCTION

THE measurement of pulsed magnetic fields is of high interest to severals sectors. Laboratory and commercial magnetic flux density meters can be found for this purpose. However, they often integrate high pass filter with a very low cut-off frequency aiming at reducing the effect of slow oscillations. In this paper we analyse the behaviour of a magnetic flux density meter largely employed for applications where the human exposure is the main concern. This meter has three selectable cut-off frequencies: 1 Hz, 10 Hz and 30 Hz. Even using the lowest one (1 Hz), possible artefact can be observed on the measured waveform. Basically, the original waveform is distorted and the degree of distortion depend on the shape of the original waveforms. The distortion could introduce unacceptable systematic error in EMC or dosimetric measurement. To give an example, complex and pulsed magnetic fields have to be assessed with suitable methodologies [1], [2], [3], [4]. This reference [5] summarises most of the available methods classifying them as time domain or frequency domain based. Different parameters are taken into account to asses the stability of the methods (offset, noise, sampling rate, signal truncation) and it is shown that some methods are more robust with reference to some disturbances and weaker with reference to others. Pros and cons of each method are highlighted. Bearing all this in mind, it is a matter of fact that a distortion of the original waveform could influence later analysis based on the measurement (e.g. an exposure assessment). This paper focuses on quasi-rectangular waveforms because they can be found in several applications like, for instance, spot welding [6], [7], [8] and MRI [9], [10], [11].

An example of a pulsed magnetic field is given in Fig. 1. The actual waveform is made of three consecutive quasi-rectangular pulses. The high pass filter distorts the actual waveform and the measurement output is the blue curve. Three main issues are clearly observed: 1) the real pulsed nature of the original waveform is lost 2) the maximum registered value is higher than the true one, 3) if the blue curve is used to compute the spectrum (apart from the filtered spectral content already discussed) it is not clear how to perform the signal truncation obtaining a result that is likely affected by spectral leakage [12], [13].

This paper addresses these issues proposing a procedure to identify the filter parameters that best reproduce the measured frequency behaviour of the meter. The model of the filter is then used to simulate the artefact related to the different cut-off frequencies. The input for the model is a reference waveform provided by the Italian reference system for the generation of standard magnetic fields up to 100 kHz [14]. The output of the model is compared with the measurement of the meter obtaining good agreement. Furthermore, it is suggested an algorithm to correct, in time domain, the distorted waveform. The correction procedure is again applied to the waveform measured by the meter obtaining a satisfactory comparison with the reference waveform. In the end, the uncertainty of the identification and correction procedure is assessed by means of the Monte Carlo method [15], [16].

II. FILTER CHARACTERISATION AND IDENTIFICATION

The experimental frequency characterisation of the magnetic field meter is carried out by using the INRIM system for the generation of standard magnetic fields up to 100 kHz [14]. A chain constituted by a Fluke 5500 calibrator and a $100\,\mathrm{A} - 100\,\mathrm{kHz}$ Clarke-Hess trans-conductance amplifier supplies the Helmholtz coil pair. The maximum magnetic flux density which can be generated in the system center is $430\,\mu\mathrm{T}$. A $24\,\mathrm{bit}$, $50\,\mathrm{kHz}$ National Instrument DAQ board performs the synchronous acquisition of the meter output signals and the current flowing in the Helmholtz system. A Python program, which manages the automatic supply frequency sweep, also performs the peak identification and the phase displacement of the meter signals (the current signal is the reference for the phase) through a four-parameter sine fitting. By replacing

L. Giaccone is with the Politecnico di Torino, Dipartimento Energia, Corso Duca degli Abruzzi 24, 10129, Torino, Italy (e-mail: luca.giaccone@polito.it)

D. Giordano and G. Crotti are with the Istituto Nazionale di Ricerca Metrologica, Strada delle Cacce 91, 10135, Torino, Italy (e-mail: d.giordano@inrim.it, g.crotti@inrim.it).
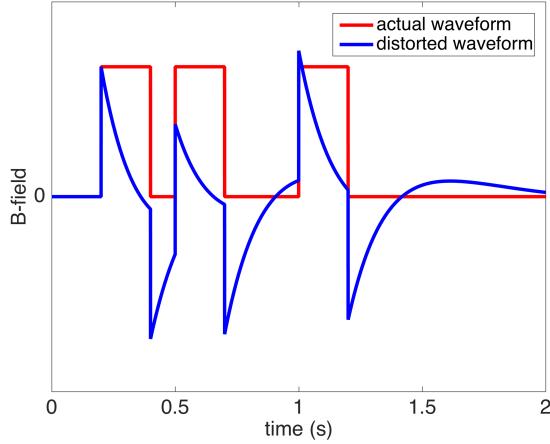
Fig. 1. Artefact example. The actual waveform is made of three consecutive quasi-rectangular pulses (red). The high pass filter distorts the actual waveform (blue).

the voltage calibrator with an arbitrary waveform generator, the system is able to generate arbitrary magnetic flux density waveforms. This allows the measurement of magnetic flux density meter capabilities under realistic distorted, quasi-rectangular or pulsed waveforms.

The magnetic field meter under study incorporates three band-pass filters with different values of the lower cut-off frequency: 1 Hz, 10 Hz and 30 Hz. The higher cut-off frequency is 400 kHz for all the filters. This paper focuses on the measurement of quasi rectangular waveforms whose spectrum includes components close to the lower cut-off frequency. For this reason, the frequency response of the magnetic field meter is characterised experimentally in the range 0.5 Hz - 300 Hz. Fig. 2 provide the measured Bode plot for the three filters. In this range they behave as a high-pass filter showing a trend similar to a third-order filter.
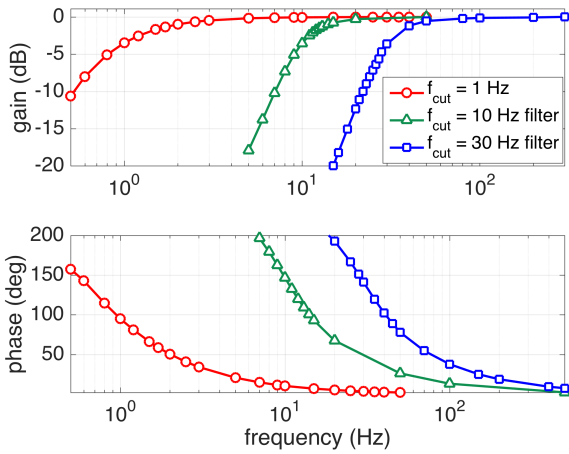

Fig. 2. Characterisation of the three filters related to the lower cut-off frequencies: 1 Hz, 10 Hz and 30 Hz.

Since the manufacturer does not provide detailed information on the band-pass filter used (only upper and lower cut-off frequency) we make the assumption that it can be modelled

by means of the third order Butterworth filter represented in Fig. 3. To identify the filter, parameters C_1, L_2 and C_3
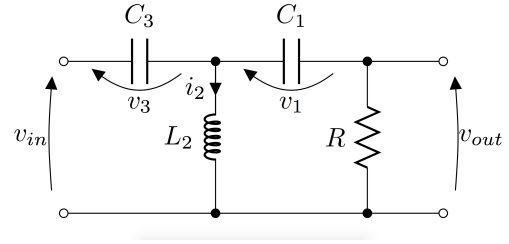

Fig. 3. Third order Butterworth filter used to approximate the actual high pass filter of the magnetic flux density meter.

have to be found. The identification is performed with a two steps approach: 1) preliminary identification with a heuristic method, 2) final identification with a deterministic method. The selected heuristic method is the genetic algorithm (GA) that allows a good exploration and exploitation of the solution space [17] but it does not assure to reach the global optimum. After the GA, the deterministic algorithm called pattern search (PS) is used in order to ensure the identification of the global optimum [18]. The PS method needs an initial solution to perform the analysis. In this paper we use as initial solution the one provided by the GA.

In both cases the algorithm minimises the mean square deviation between Butterworth and measured gain. The objective function is defined as:

$$\text{OF} = \sqrt{\sum_j \left(G_{\text{j,B}} - G_{\text{j,mes}} \right)^2} \tag{1}$$

being:

- j the index of the jth frequency,
- $G_{\text{j,B}}$ the gain of the Butterworth filter at the jth frequency,
- $G_{\text{j,mes}}$ the measured gain of the meter filter at the jth frequency.

The OF does not use information about the phase and, hence, they have to be checked at the end of the process (as will be shown later).

The whole process is run several times to check the stability of the final results. It is found that the use of the two steps approach makes the identification really stable and independent of the GA parameters used (population size, crossover, mutation factors). Such parameters can only influence the elapsed time but not the final result that always converges to the same optimal values. It must be stressed, however, that the GA has the key role of identifying the local optimum used by the PS as initial solution. Without this information the procedure can fail leading to a non global optimum.

The optimal parameters are summarised in Table I for all the filters. Fig. 4 compares the frequency characterisation of the meter and the Butterworth filter frequency response obtained with the identification. For the sake of shortness, this comparison is provided only for the lowest cut-off frequency ($f_{\text{cut}} = 1$ Hz). It is apparent that the Butterworth filter approximates the actual filter with good agreement. A slightly

higher error is found for the phase at lower frequencies. This deviation is likely caused by the main assumption that approximates the actual filter with a Butterworth filter. However, we will shown later that this deviation does not compromise the final goal of our analysis.

TABLE I
OPTIMAL PARAMETERS OF THE BUTTERWORTH FILTER

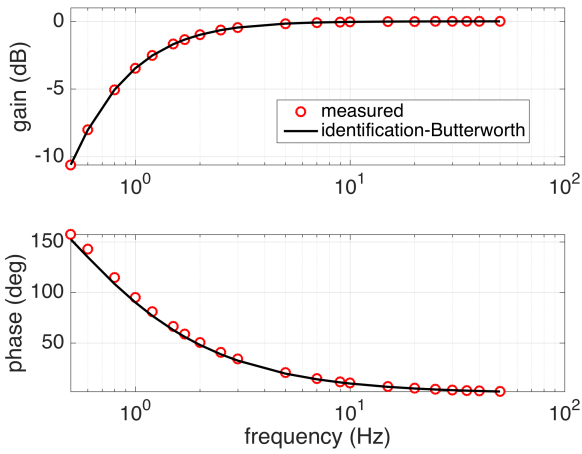| parameter	optimal value $f_{\text{cut}} = 1$ Hz	optimal value $f_{\text{cut}} = 10$ Hz	optimal value $f_{\text{cut}} = 30$ Hz
C_1	675.06 mF	33.70 mF	10.02 mF
L_2	236.79 mH	10.36 mH	3.76 mH
C_3	106.73 mF	10.56 mF	3.35 mF

Fig. 4. Result of the fitting with cut-off frequency equal to $f_{\text{cut}} = 1$ Hz. Measured frequency response vs. Butterworth frequency response.

III. ARTEFACT MODELLING

The robustness of the identification is tested trying to reproduce the measurement artefacts. The same system described in Sec. II is used to generate a quasi-rectangular periodic waveform with fundamental frequency of 10 Hz. Fig. 5 shows the magnetic flux density waveform together with its spectrum. It is apparent that, depending on the filter used, a significant portion of the spectrum is attenuated of even cancelled. The reference waveform is measured by a fluxgate magnetometer and it will be used for comparison in the rest of the paper.

The modelling of the artefacts is performed solving a system of three differential equations related to the Butterworth in Fig. 3:

$$\frac{\mathrm{d}v_1}{\mathrm{d}t} = \frac{v_{\text{in}} - v_1 - v_3}{RC_1} \tag{2}$$

$$\frac{\mathrm{d}i_2}{\mathrm{d}t} = \frac{v_{\text{in}} - v_3}{L_2} \tag{3}$$

$$\frac{\mathrm{d}v_3}{\mathrm{d}t} = \frac{v_{\text{in}} - v_1 - v_3}{RC_3} + \frac{i_2}{C_3} \tag{4}$$

In equations (2), (3) and (4) the term v_{in} corresponds to the reference field waveform represented in Fig. 5. Once the three
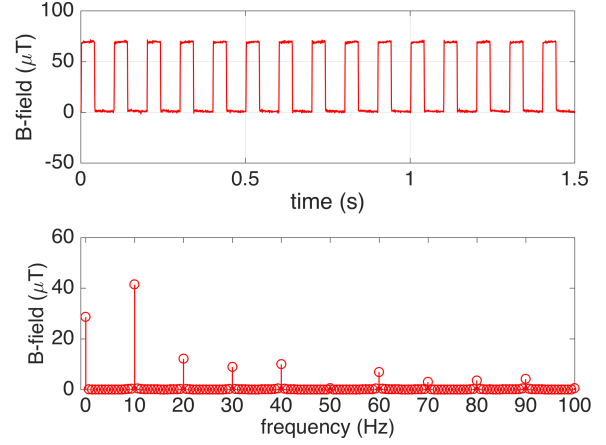

Fig. 5. Quasi-rectangular periodic waveform with fundamental frequency of 10 Hz (a). Spectrum of the waveform. (b).

differential equation are solved, one can compute the output voltage as $v_{\text{out}} = v_{\text{in}} - v_1 - v_3$. This term corresponds to the magnetic flux density waveform distorted by the meter.

Simulations are performed for all the filters incorporated in the meter. Results are provided in Fig. 6, Fig. 7 and Fig. 8 for the cut-off frequencies of 1 Hz, 10 Hz and 30 Hz, respectively. The red curve is the reference waveform, the green curve is the waveform measured by the meter and the blue (dashed) one is the simulation. In all figures three cycles are magnified to make easier the comparison. It is apparent that a good agreement is found for all the filters.
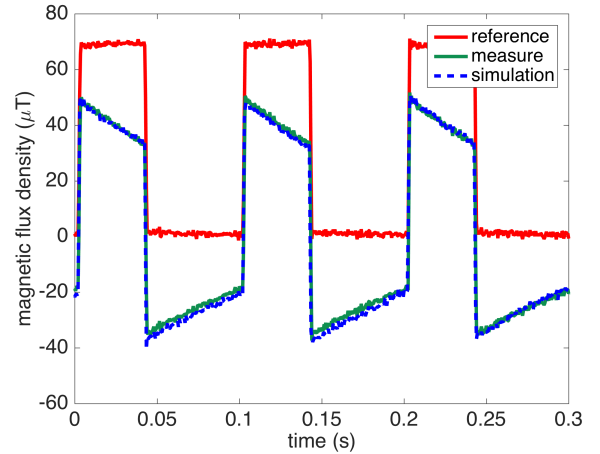

Fig. 6. Simulation of the measurement artefact related to $f_{\text{cut}} = 1$ Hz. The red curve is the reference waveform, the green curve is the waveform measured by the meter and the blue (dashed) curve is the simulation.

IV. CORRECTION PROCEDURE

In this section the attention is focused on a more interesting aspect related to the use of the identified filters. Since the identification has been proven to be reliable in previous sections, one can attempt to use it for the correction of the
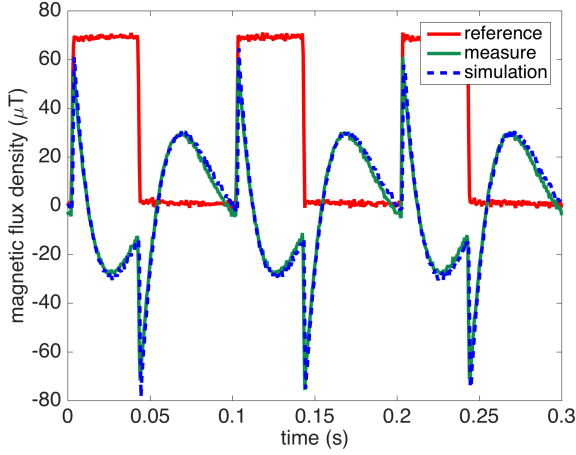
Fig. 7. Simulation of the measurement artefact related to $f_{cut} = 10$ Hz. The red curve is the reference waveform, the green curve is the waveform measured by the meter and the blue (dashed) curve is the simulation.

Fig. 8. Simulation of the measurement artefact related to $f_{cut} = 30$ Hz. The red curve is the reference waveform, the green curve is the waveform measured by the meter and the blue (dashed) curve is the simulation.
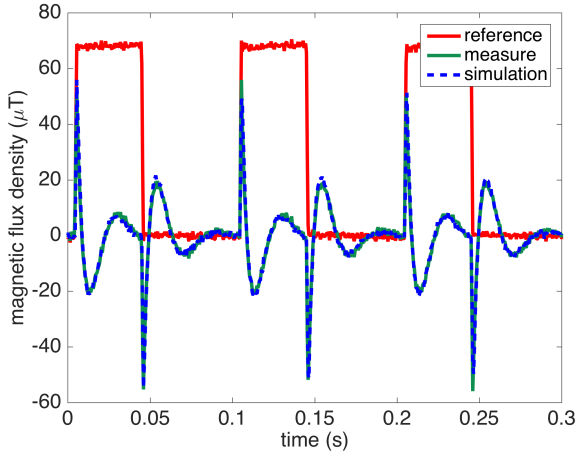
distorted waveform obtaining the true one (without artefacts). The set of equations necessary to the correction are:

$$\frac{\mathrm{d}v_1}{\mathrm{d}t} = \frac{v_{out}}{RC_1} \tag{5}$$

$$\frac{\mathrm{d}i_2}{\mathrm{d}t} = \frac{v_1 + v_{out}}{L_2} \tag{6}$$

$$\frac{\mathrm{d}v_3}{\mathrm{d}t} = \frac{v_{out}}{RC_3} + \frac{i_2}{C_3} \tag{7}$$

It is noteworthy that, unlike to the simulation of the artefact, these equations can be decoupled. Equation (5) can be solved independently by the others obtaining v_1. This voltage is used to solve equation (6) and the obtained results can be used, in the same way, for solving (7). Once the three differential equation are solved, one can compute the input voltage as $v_{out} = v_{out} + v_1 + v_3$, where, v_{out} is the field waveform distorted by the meter and v_{in} is the corrected magnetic flux density waveform.

When solving equations from (5) to (7) particular attention has to be paid to the possibility of having a mean value in the waveforms v_{out}. The effect of the high-pass filter included in the meter is the cancellation of the mean value in the output waveform. For the quasi-rectangular waveform under analysis the mean value is completely cancelled after one single cycle. During the correction process one has to select a portion of the waveform that does not present a mean value, otherwise the three sequential integral will lead to waveform that varies with the third power of the time superposed on true waveform. Finally, technically speaking, even after the selection of a waveform without a mean value, it is better to numerically remove possible very small mean values coming from the signal truncation.

A. Correction procedure applied to quasi-rectangular waveforms

The correction procedure has been successfully applied to the measured waveforms presented in previous section. Fig. 9, Fig. 10 and Fig. 11 provide the comparison for the cut-off frequencies of 1 Hz, 10 Hz and 30 Hz, respectively. They all include the reference waveform (red), the waveform measured by the meter (green), and the corrected waveform in (blue, dashed). It is worth noting that the correction procedure based on the removal of the mean values provides, obviously, a result without a mean value as well. The corrected waveforms presented in figures from 9 to 11 are obtained imposing, at the end of the correction process, that the waveform starts from zero.
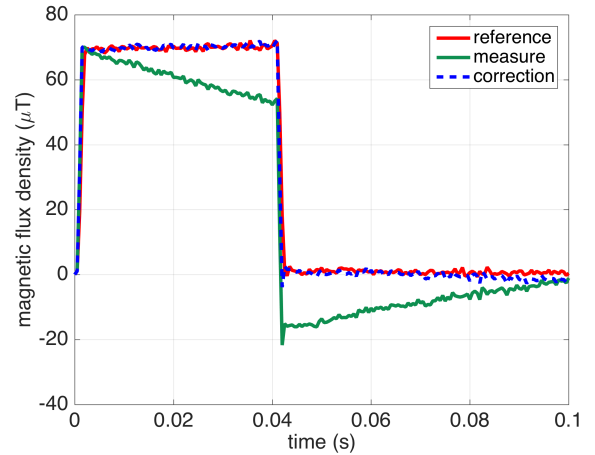

Fig. 9. Test of the correction procedure on the measured waveform with $f_{cut} = 1$ Hz. The red curve is the reference waveform, the green curve is the waveform measured by the meter and the blue (dashed) curve waveform obtained by means of the correction procedure.

B. Correction procedure applied to a real case study: MFDC spot welding gun

The correction procedure is finally tested on a magnetic flux density waveform measured close to a medium frequency direct current welding gun. The magnetic field is pulsed and the highest frequency of the spectrum is approximately
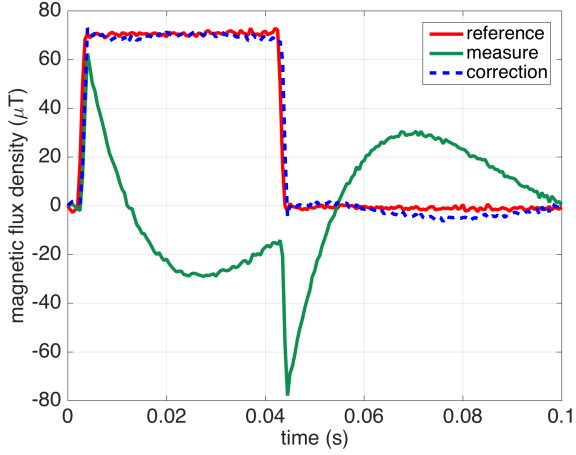
Fig. 10. Test of the correction procedure on the measured waveform with $f_{cut} = 10$ Hz. The red curve is the reference waveform, the green curve is the waveform measured by the meter and the blue (dashed) curve waveform obtained by means of the correction procedure.

Fig. 11. Test of the correction procedure on the measured waveform with $f_{cut} = 30$ Hz. The red curve is the reference waveform, the green curve is the waveform measured by the meter and the blue (dashed) curve waveform obtained by means of the correction procedure.
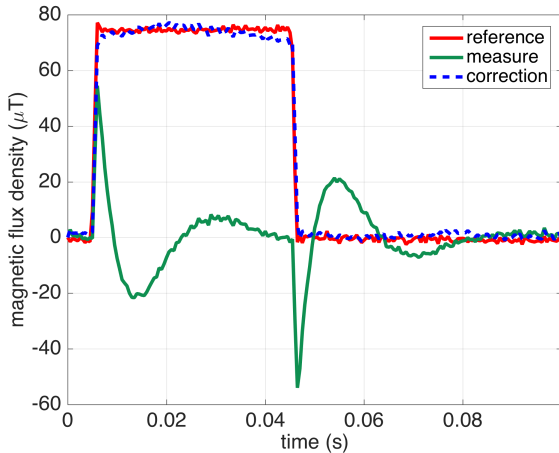
10 kHz [7]. This kind of waveform is clearly subject to the measurement issues described in this paper. Fig. 12 provides in red the measured waveform using the filter with the lowest cut-off frequency, $f_{cut} = 1$ Hz. By processing this waveform with the correction procedure the blue curve is obtained. The lowest subfigure magnifies the time range during the slope-up of the magnetic flux density in order to appreciate the quality of the correction.

From the technical point of view, the blue curve is obtained removing the mean value before the integration in time domain. The result is then shifted up knowing that the waveform starts from zero. This knowledge comes from the fact that the magnetic flux density is proportional to the welding current that was measured as well during the pulse.
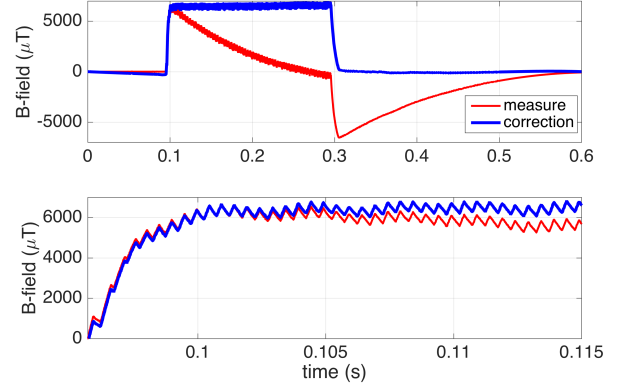

Fig. 12. Correction of the magnetic flux density waveform generated by a welding gun. Measurement in red and correction in blue.

V. UNCERTAINTY

The uncertainty associated to the standard deviation between the measured and corrected magnetic flux density signals can be estimated by a applying a Monte Carlo method (MCM) [15], [16]. The correction procedure is based on the identification of the filter parameters and, consequently, on the measurement of the frequency characterisation of the filter (gain and phase). The MCM is applied to the following model: 1) identification of the filter, 2) application of the correction procedure, 3) computation of the mean square error between correction and reference signal. Since the inputs of the MCM come from a measurement procedure, the associated probability density function (pdf) has a gaussian shape.

It is important to highlight that the pdf associated with the MCM output actually involves both the output of the propagated uncertainty of the complex transfer function and the repeatability of the identification stage of the model. Moreover, the obtained information is only a part of the overall uncertainty associated with the magnetic flux density quantity, which is the actual measurand. In a complete uncertainty budget, the meter uncertainty, the actual environmental conditions, the magnetic flux density uniformity, etc... have to be considered. This analysis is out of our aim.

In the estimation of the uncertainty associated with the gain and phase of the filter only a type A uncertainty is considered. The setup and the procedure employed is able to estimate the ratio and the phase displacement between two sinusoidal waveforms showing an uncertainty of few tens of μV/V and few tens of μrad. Nevertheless, because of the noise associated with the acquired voltage proportional to the magnetic flux density, the repeatability quantified by the standard deviation computed over a population of 50 repeated measurements gives a mean value of about 0.3 % for the gain (computed over the whole frequency bandwidth). Finally, since the identification does not rely on the measurement of the phase (see the objective function definition in Sec. II) it is not considered in the MCM.

The Monte Carlo analysis is performed on 20000 draws, considering a standard deviation of the measured gain of 0.3 %. As a result, the probability density function of the

output is shown in Fig. 13. The best fitting of this distribution with a gaussian shape provides a mean value of 8.63 μT with a standard deviation of 0.065 μT that means 0.75 %.

The same analysis is used also to evaluate the uncertainty of the identification procedure. At each run of the MCM the value of C_1, L_2 and C_3 is registered. The best fitting of their distribution with a gaussian shape provides the results summarised in Table II. The same table summarises also the results for the mean square error presented above.
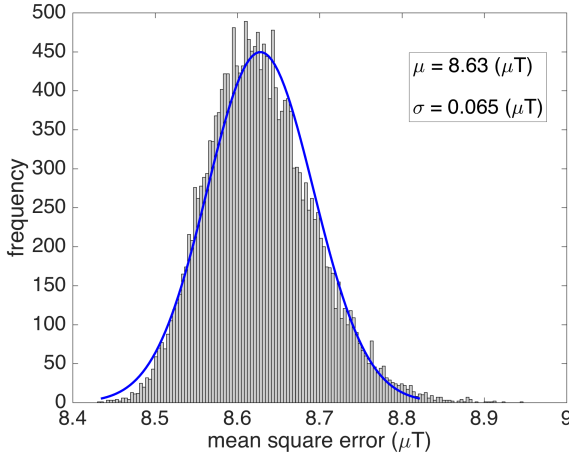

Fig. 13. Probability density function of the mean square error related to the correction procedure. The best fitting of this distribution with a gaussian shape provides a mean value of 8.63 μT with a standard deviation of 0.065 μT that means 0.75 %.

TABLE II
UNCERTAINTY OF IDENTIFICATION AND CORRECTION PROCEDURE

parameter	mean μ	standard deviation σ	standard deviation (%)
C_1	675.36 mF	21.47 mF	3.179
L_2	236.89 mH	2.06 mH	0.870
C_3	106.73 mF	0.18 mF	0.169
MSE	8.63 μT	0.065 μT	0.753

VI. CONCLUSION

When an AC magnetic flux density meter is employed in the detection of pulsed signals, time domain artefact can occur. This could introduce unacceptable systematic error in EMC or dosimetric measurement purposes. In this paper we extend the preliminary work presented in [19]. We analyse the behaviour of a magnetic flux density meter largely employed for applications where the human exposure is the main concern. This meter has three selectable cut-off frequencies: 1 Hz, 10 Hz and 30 Hz. The three filters are characterised showing the classical trend of a third order high pass filter. We propose an identification procedure based on a two steps approach (heuristic + deterministic) that is shown to be effective and reliable. The identified parameters allow to accurately model the meter behaviour and to develop a correction procedure that makes possible to compute the true waveform starting

from the measured (distorted) one. The correction procedure is tested with two different waveforms: 1) a quasi-rectangular periodic waveform provided by a system for the generation of standard magnetic fields, 2) a pulsed waveform generated by a spot welding device. In both cases a satisfactory correction is obtained.

Finally, the uncertainty of the identification and correction procedure is evaluated by means of the Monte Carlo method. Starting from the frequency characterisation of the filter affected by a standard uncertainty of 0.3 % it is found a standard uncertainty of the correction procedure of 0.75 % which correspond to an expanded uncertainty of 1.5% (coverage factor = 2). This figure, which has to be considered as a contribution to the uncertainty budget associated with on-site magnetic flux density measurement, gives a negligible contribution compared with the expanded uncertainty which generally is around 10%.

REFERENCES

[1] K. Jokela, "Restricting exposure to pulsed and broadband magnetic fields," *Health Phys*, vol. 79, no. 4, pp. 373–388, 2000.
[2] ICNIRP, "Guidance on determining compliance of exposure to pulsed and complex non-sinusoidal waveform below 100 kHz with icnirp guidelines," *Health Phys*, vol. 84, no. 3, pp. 383–387, 2003.
[3] ICNIRP, "Guidelines for limiting exposure to time-varying electric and magnetic fields (1 Hz to 100 kHz)," *Health Phys*, vol. 99, no. 6, pp. 818–836, 2010.
[4] "Non-binding guide to good practice for implementing Directive 2013/35/EU - Electromagnetic Fields - Volume 1: Practical Guide," ISBN: 978-92-79-45869-9, DOI: 10.2767/961464, 2015.
[5] V. De Santis, X. L. Chen, I. Laakso, and A. Hirata, "On the issues related to compliance of LF pulsed exposures with safety standards and guidelines," *Phisycs in Medicine and Biology*, vol. 58, pp. 8597–8607, 2013.
[6] A. Canova, F. Freschi, L. Giaccone, and M. Repetto, "Exposure of working population to pulsed magnetic fields," *IEEE Transaction on Magnetics*, vol. 46, no. 8, pp. 2819–2822, 2010.
[7] A. Canova, F. Freschi, L. Giaccone, and M. Manca, "A simplified procedure for the exposure to the magnetic field produced by resistance spot welding guns," *IEEE Transaction on Magnetics*, vol. 52, no. 3, art. num 5000404, 2016.
[8] "EN 50505 - Basic standard for the evaluation of human exposure to electromagnetic fields from equipment for resistance welding and allied processes."
[9] F. Hennel, F. Girard, and T. Loenneker, ""Silent" MRI with soft gradient pulses," *Magnetic resonance in medicine*, vol. 42, pp. 6–10, jul 1999.
[10] H. Han, A. V. Ouriadov, E. Fordham, and B. J. Balcom, "Direct measurement of magnetic field gradient waveforms," *Concepts in Magnetic Resonance Part A*, vol. 36A, pp. 349–360, nov 2010.
[11] D. Giordano, M. Borsero, G. Crotti, and M. Zucca, "Analysis of magnetic and electromagnetic field emissions produced by a MRI device," *Proc. 17th Symp. Imeko TC4*, p. 86.
[12] T. Grandke, "Interpolation Algorithms for Discrete Fourier Transforms of Weighted Signals," *IEEE Transactions on Instrumentation and Measurement*, vol. 32, pp. 350–355, jun 1983.
[13] D. Bellan, A. Gaggelli, F. Maradei, A. Mariscotti, and S. Pignari, "Time-Domain Measurement and Spectral Analysis of Nonstationary Low-Frequency Magnetic-Field Emissions on Board of Rolling Stock," *IEEE Transactions on Electromagnetic Compatibility*, vol. 46, pp. 12–23, feb 2004.
[14] M. Chiampi, G. Crotti, and D. Giordano, "Set up and characterization of a system for the generation of reference magnetic fields from 1 to 100 kHz," *Instrumentation and Measurement, IEEE Transactions on*, vol. 56, no. 2, pp. 300–304, 2007.
[15] Joint Committee for Guides in Metrology, "JCGM 101 – Evaluation of measurement data – Supplement 1 to the "Guide to the expression of uncertainty in measurement" – Propagation of distributions using a Monte Carlo method (ISO/IEC Guide 98-3-1)," 2008.

[16] O. Bottauscio, M. Chiampi, G. Crotti, D. Giordano, W. Wang, and L. Zilberti, "Uncertainty estimate associated with the electric field induced inside human bodies by unknown lf sources," *IEEE Transactions on Instrumentation and Measurement*, vol. 62, pp. 1436–1442, June 2013.

[17] J. H. Holland, *Adaptation in Natural and Artificial Systems*. Ann Arbor, MI: The Univ. of Michigan Press, 1975.

[18] R. Hooke and T. A. Jeeves, ""Direct search" solution of numerical and statistical problems," *Journal of the Association for Computing Machinery*, vol. 8, no. 2, pp. 212–229, 1961.

[19] G. Crotti, L. Giaccone, and D. Giordano, "Identification and correction of artefact in the measurement of pulsed magnetic fields," in *Conference on Precision Electromagnetic Measurements, CPEM, Ottawa, Canada*, 10-15 July 2016.

Domenico Giordano received the Ph.D. degree in electrical engineering from the Politecnico of Torino, Torino, Italy, in May 2007. From 2007 to 2009, he collaborated with Istituto Nazionale di Ricerca Metrologica (INRIM), Torino, with a postdoctoral research grant. Since 2009, he has been with the Electromagnetics Division, INRIM. His research interests include the evaluation of human exposure to magnetic fields generated by nonsinusoidal and impulsive sources and studies of procedures for the calibration of magnetic field meters, on the study of ferroresonance phenomena and on the development and characterization of voltage transducers for on-site calibration and power quality measurements on the medium-voltage grid.

Luca Giaccone (SM'15) was born in Cuneo, Italy, in 1980. He received the Laurea degree and the Ph.D. degree in Electrical Engineering from the Politecnico di Torino, Turin, Italy, in 2005 and 2010, respectively. Dr. Giaccone worked on several areas of the electrical engineering: optimisation and modelling of complex energy systems, computation of electromagnetic and thermal fields, energy scavenging, magnetic field mitigation, EMF dosimetry, compliance of LF pulsed magnetic field sources. Since 2011 he is assistant professor with the Politecnico di Torino, Dipartimento Energia. He is member of the IEEE since 2014 and he has been elevated to senior member in February 2015. Since November 2015 he is member of the IEEE International Committee on Electromagnetic Safety - TC 95 - SC6 EMF Dosimetry Modeling.

Gabriella Crotti received the M.S. degree in physics from the University of Torino, Torino, Italy, in 1986. She is a Chief Technologist in the Electromagnetics Division, Istituto Nazionale di Ricerca Metrologica (INRIM), Torino. Her research interests include the development of references and measurement techniques of high voltages, high currents, and low and intermediate-frequency electromagnetic fields.